Explanation of Bubble Nucleation Mechanisms: A Gradient Theory Approach

Kurian J. Vachaparambil [z] **and Kristian Etienne Einarsrud**

Department of Materials Science and Engineering, Norwegian University of Science and Technology (NTNU), Trondheim 7491, Norway

A Helmholtz free energy description of the four nucleation mechanisms used to explain the bubble nucleation in electrochemical systems is presented. The mechanisms are compared based on the nucleation energy barrier and critical nuclei radius. The theoretical analysis sheds light on the effect of parameters like contact angle on the electrode surface and pre-existing gas bubbles on nucleation energy barrier. A free energy based description of surface tension (planar interface) is also obtained from the thermodynamic framework.

 [DOI: 10.1149/2.1031810jes]

Manuscript submitted May 14, 2018; revised manuscript received July 3, 2018. Published July 24, 2018. This was Paper 1366 presented at the Seattle, Washington Meeting of the Society, May 13–17, 2018.

The phenomenon of nucleation is a thermodynamic process that governs phase separation in both natural and technological processes, like bubble formation in electrochemical systems. Nucleation is affected by both temperature and supersaturation level of the liquid. When nucleation is influenced by temperature, like in case of boiling, the change in temperature causes changes in local pressure that favors formation of vapor nuclei.[1] In supersaturated systems, however, the nucleation happens because of the system's attempt to recover equilibrium by phase separation at a constant temperature. Gas evolution on electrodes is a good example of nucleation driven by supersaturation, the continuous redox reactions on the electrodes leading to supersaturation of the liquid with gas, promoting the formation of the gas bubble. The common features and disparity between temperature driven gas evolution like boiling and electrochemical gas evolution, including bubble nucleation, has been highlighted in the work by Vogt et al.[2]

Four mechanisms proposed by Jones et al.,[3] are used to describe the experimental observations for gas bubble nucleation in supersaturated systems:

- Type 1 or homogeneous nucleation occurs in the liquid bulk at high levels of supersaturation;
- Type 2 or heterogeneous nucleation happens at surface imperfections like pits and cavities at lower levels of supersaturation compared to Type 1;
- Type 3 or pseudo-classical nucleation utilizes pre-existing gas cavities that have radii smaller than the critical radius predicted by the classical theory to lower the nucleation energy barrier (compared to Types 1 and 2);
- Type 4 or non-classical nucleation occurs at pre-existing gas cavities whose radii is larger than the critical radius, effectively reducing the energy barrier to zero.

The pre-existing gas cavities, relevant in Type 3 and 4 mechanisms, can occur from previous nucleation,[4] entrainment of gas from liquid jet[5] and solid surface trapping gases.[6] Nanobubbles, whose radii is smaller than the critical radius,[7] adhering to the solid surface could also facilitate nucleation.

In the work by German et al., homogeneous and heterogeneous nucleations are considered to drive the gas bubble nucleation from a platinum nanodisk.[8] The paper by Sequeira et al., reviewed existing experimental work where the electrode surface assisted the gas nucleation in electrochemical systems.[9] According to Taqieddina et al., nucleation of gas bubbles in electrochemical reactors is assisted by solid surfaces and pre-existing gas bubbles.[10] While modeling electrochemical systems, the proposed nucleation appears to be based on Type 4 as the nucleation energy barrier is seldom considered.[11,12] Generally, the energy requirement for gas bubble nucleation (Types 1 and 2) is done based on maximization of Gibbs and Helmholtz free energy difference of the system before and after nucleation.[13,14] In the general analysis of electrochemical systems, the surface tension between the gas bubble and the surrounding liquid is typically considered to be constant.[11,15] The presence of dissolved gas in the liquid has been proposed to change this surface tension by Lubetkin,[16] and observed in molecular dynamics simulation.[17] The change in surface tension is critical in electrochemical systems where supersaturation drives the nucleation.

The main aim of the paper is to provide a macroscopic thermodynamic explanation for the nucleation energy requirement for the four nucleation mechanisms proposed by Jones et al.[3] Although classical nucleation theories have explained the nucleation energy requirement for Type 1 and Type 2 nucleation from a Gibbs approach,[18] Type 3 and Type 4 nucleation modes, used in practical modeling of electrochemical systems, to the best of the author's knowledge has not been investigated yet. This paper uses the Helmholtz free energy description developed by Cahn and Hilliard (C-H), to study interfacial energy and nucleation,[19,20] instead of the classical approach like Gibbs which is typically used for nucleation and interface studies.[18,21] The nucleation energy barrier and critical radius calculated by this method is compared against the results of Type 1 and Type 2 mechanisms from classical nucleation theories. The framework is then used to derive the critical radius and nucleation energy barrier of Type 3 and Type 4 mechanisms.

Gas nucleation and evolution is very important in electrochemical systems where the gas can either be a product (electrolysis, chloroalkali processes) or a by-product (aluminum production) of the process at hand, but is in all cases linked to the overall performance of the system. Usually gas evolution is a term used to describe the process which begins with bubble nucleation, followed by bubble growth and detachment from the electrode surface.[22] The presence of bubbles on the electrode surface reduces the area of the electrode in contact with the electrolyte, which reduces the efficiency of the electrochemical system. Experimental work has also shown that gas evolution on the electrode adversely effects the catalyst coating.[23,24] The work by Kadyk et al. showed that the use of preferential nucleation sites can reduce the damage done to the catalyst coating and electrode surface, thus increasing the durability and efficiency of electrodes.[25] Understanding nucleation can thus provide insight on how bubble generation can be controlled and identify plausible nucleation sites to design more durable and efficient electrodes.

Thermodynamic Definitions

Once a solution has reached supersaturation, nucleation reduces the local supersaturation levels, which is observed as effervescence

[z]E-mail: kurian.j.vachaparambil@ntnu.no

in carbonated beverages. In electrochemical systems, the continuous surface reactions on the electrodes maintains the electrolyte at a constant supersaturation level. The number of gas molecules that phase separates can be considered to be much smaller than the total number of molecules in the volume encompassing both the bubble and electrolyte (henceforth referred to as system). This approximation is valid when the reactions at the electrodes are instantaneous and the nucleated bubble does not grow in the reaction time. The volume of the nucleated bubble can also be neglected in comparison to the total volume of the system.[26] By neglecting the effects of temperature to assume a fixed system volume, Helmholtz free energy can be used instead of Gibbs energy to describe the thermodynamics of the system.[26,27]

The C-H model, based on the studies on interface and nucleation,[19,20] combined with fluid flow equations (diffuse-interface method) has proven useful in simulating multiphase flows.[28,29] The C-H model has also been successfully used to numerically model the nucleation process where the nucleated particle size is a few nanometers.[30] A more recent work by Lee et al.[26] which provides a physical and mathematical derivation of the binary C-H equation is also useful in understanding the free energy formulations in this paper.

The thermodynamic definitions used in this paper is based on C-H paper which delves into the interface physics.[19] This formulation of the free energy is used due to its relative simplicity compared to frameworks like Gibbs and Guggenheim.[21] The possible states in which the constituent molecules can exist is denoted using the following: solution of liquid (L) and dissolved gas which is henceforth referred to as mixture is represented as M, interface is I and bubble is denoted by G. For a given state i, the free energy per unit volume is represented as F_i^0 and the mole fraction of the component in i is denoted by χ_i.

The free energy per unit volume in an arbitrary volume (v) in the system can be written as

$$F_v^0 = F_{mix}^0 + k|\nabla\chi_L|^2, \qquad [1]$$

where the first term is the contribution due to local mixing (further described by Eq. 2) and the second term is due to the presence of gradients in the system.[19] $\nabla\chi_L$ which is the spatial gradient of the liquid mole fraction and k is constant for a given system.[19,26] The free energy per unit volume of pure liquid and gas is given by F_L^0 and F_G^0 respectively. When the liquid and the gas is mixed, the inter-molecular bonds change due to the presence of dissimilar molecules along with an increase in entropy. The free energy per unit volume of the mixture of gas and liquid as

$$F_{mix}^0 = (1-\chi_L)F_G^0 + \chi_L F_L^0 + \Delta F^0, \qquad [2]$$

where the first two terms represent the free energy per unit volume due to ideal mixing and ΔF^0 represent the change because of the mixing of gas and liquid.[26]

The interface is considered as a region of finite volume where the transition from physical properties of mixture to bubble, occurs over a very small interface thickness (as illustrated in Fig. 1). Typically, the concentration variation across the interface is modeled as a sigmoid function which has been observed to correspond to actual interface structure.[31] The boundaries of the interface are set at locations along the radial direction such that the local composition remains constant further into the bulk (mixture or bubble). Although the regions of the mixture and bubble close to the interface tend to slightly deviate from the bulk composition, for all practical purposes this deviation can be neglected and composition can be approximated to be close to the asymptotic composition. By setting discrete positions to define the region for the interface, allows the thermodynamic terms to be integrated separately for the mixture, bubble and interface.

The free energy per unit volume of the mixture is given as F_M^0 while the corresponding term for the bubble is F_G^0. Both these terms are calculated by substituting the corresponding value of χ_L from Fig. 1 and neglecting the gradient term in Eq. 1 (because of the constant composition in the bulk). The free energy per unit volume of the interface region is

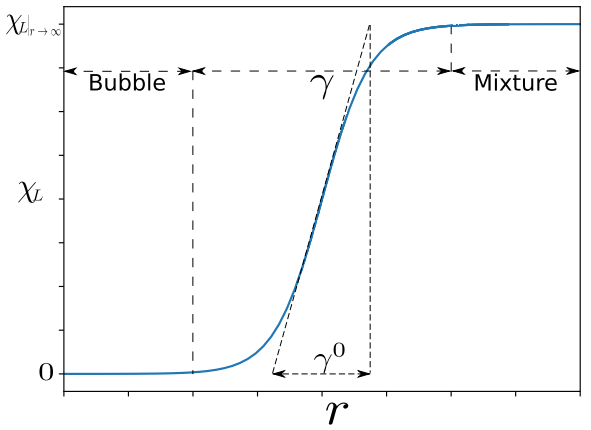

Figure 1. Schematic of the variation in mole fraction of liquid (χ_L) across an interface of thickness γ between mixture and bubble. The interface thickness used in C-H theory (γ^0) is smaller than the interface thickness used in this paper.

$$F_I^0 = k|\nabla\chi_L|^2 + F_{mix}^0, \qquad [3]$$

based on terms introduced in Eq. 1. The contributions to F_I^0 contains the free energy due to the gradient of composition across the interface and mixing (locally) within the interface. The work by C-H[19] calculates the interfacial free energy of a system with no supersaturation but another study by the same authors on nucleation in a supersaturated system[20] uses a different formulation (that uses an additional term for the supersaturation in the mixture) to ensure that the interfacial free energy is non-zero only within the interface. Since Eq. 3 is based on C-H,[19] it does not account for the effect of supersaturation of the mixture on the interfacial free energy. The volume integral of F_I^0 over the interface volume (V_I) is dealt with as

$$\int_{V_I} F_I^0 dV = V_I \overline{F_I^0}. \qquad [4a]$$

In the above equation, $\overline{F_I^0}$ can be interpreted as volume averaged free energy of the interface when the effect of the supersaturated is not considered. Similarly, volume integrals of F_M^0 and F_G^0 are treated as

$$\int_{V_M} F_M^0 dV = V_M \overline{F_M^0},$$
$$\int_{V_G} F_G^0 dV = V_G \overline{F_G^0}. \qquad [4b]$$

Analysis of Nucleation Mechanisms

In this section, the thermodynamic favorability of each nucleation mechanism is discussed in detail. The annotation used in this paper to denote homogeneous, heterogeneous, pseudo-classical and non-classical nucleation mechanisms are $T1$, $T2$, $T3$ and $T4$ respectively.

Type 1 or homogeneous nucleation ***($T1$).***—Fig. 2 shows a schematic of the homogeneous nucleation process in an electrochemical system with Fig. 2a representing the mixture (supersaturated liquid) in contact with the electrode surface before the onset on nucleation, while Fig. 2b shows the bubble formed in the bulk of the solution. The nucleated bubble is assumed to have an inner radius of R which can be used to defined the volume of the gas bubble (V_G),

$$V_G = \frac{4}{3}\pi R^3. \qquad [5]$$

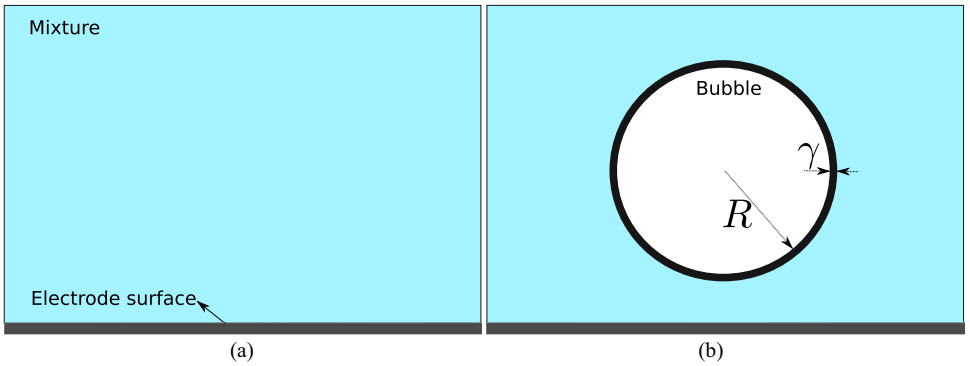

Figure 2. Schematic of homogeneous nucleation. (a) Before nucleation (b) After nucleation.

Due to the finite interface thickness γ, outer radius of the interface is $R+\gamma$. The volume of the interface V_I is

$$V_I = \frac{4}{3}\pi\Big((R+\gamma)^3 - R^3\Big). \quad [6]$$

Usually, γ is very small and generally in the order of few angstroms.[32] In comparison, the radius of the nucleated bubble is usually in nanometers.[33] So the interface thickness can be approximated as $\gamma << R$ and volume of the interface (Eq. 6) can be simplified to Eq. 7, where A_{MG} is the area of the mixture-gas interface in a spherical bubble (is the limiting case of a sharp interface),

$$\lim_{\gamma/R\to 0} V_I = 4\pi\gamma R^2 = \gamma A_{MG}. \quad [7]$$

The free energy of the system before nucleation (F_1^*) can be written as

$$F_1^* = \int_{V_0} F_M^0 dV + \int_{A_0} \sigma_{SM} dA, \quad [8]$$

where V_0 is the total volume of the solution before nucleation, F_M^0 free energy of the mixture (liquid and dissolved gas) per unit volume and σ_{SM} is the interfacial tension in the limit of a sharp (zero thickness) solid-mixture interface. The integral involving σ_{SM} is the energy attributed to the surface tension at the area where solid and mixture are in contact (A_0). After nucleation, the free energy of the system (F_2^*) is

$$F_2^* = \int_{V_0-V_I-V_G} F_M^0 dV + \int_{V_I} F_I^0 dV + \int_{V_G} F_G^0 dV + \int_{A_0} \sigma_{SM} dA, \quad [9]$$

where the second and third term is the free energy of the interface and gas bubble respectively. Subtracting Eq. 8 and Eq. 9 gives the change in the free energy of the system before and after nucleation (ΔF_{T1}^*),

$$\Delta F_{T1}^* = \int_{V_0-V_I-V_G} F_M^0 dV + \int_{V_I} F_I^0 dV + \int_{V_G} F_G^0 dV - \int_{V_0} F_M^0 dV. \quad [10]$$

The volume integrals of free energies per unit volume (F_M^0, F_I^0 and F_G^0) are treated as shown in Eq. 4, and Eq. 10 can be simplified as

$$\Delta F_{T1}^* = V_I\Big(\overline{F_I^0} - \overline{F_M^0}\Big) + V_G\Big(\overline{F_G^0} - \overline{F_M^0}\Big). \quad [11]$$

Substituting the volume of gas bubble and interface from Eq. 5 and Eq. 7 into Eq. 11,

$$\Delta F_{T1}^* = 4\pi\gamma R^2\Big(\overline{F_I^0} - \overline{F_M^0}\Big) + \frac{4}{3}\pi R^3\Big(\overline{F_G^0} - \overline{F_M^0}\Big), \quad [12]$$

where the first term represents the interfacial surface energy and the subsequent term corresponds to volumetric energy. The critical radius R_c for nucleation can be calculated from $d\Delta F_{T1}^*/dR = 0$,

$$R_c = -\frac{2\gamma\Big(\overline{F_I^0} - \overline{F_M^0}\Big)}{\overline{F_G^0} - \overline{F_M^0}}. \quad [13]$$

The critical radius described in Eq. 13, is analogous to critical radius predicted by classical nucleation theory ($R_c = 2\sigma_{MG}/\Delta G_v$),[18] which gives

$$\sigma_{MG} = \gamma\Big(\overline{F_I^0} - \overline{F_M^0}\Big),$$
$$\Delta G_v = \overline{F_M^0} - \overline{F_G^0}, \quad [14]$$

where σ_{MG} and ΔG_v are the surface tension at the mixture-bubble interface and free energy change per unit volume associated with nucleation respectively.

For the nucleation mechanism to maximize the change in free energy of the system, $d^2\Delta F_{T1}^*/dR^2|_{R=R_c} < 0$ should be satisfied, where R_c is defined in Eq. 13,

$$\left.\frac{d^2\Delta F_{T1}^*}{dR^2}\right|_{R=R_c} = 8\pi\gamma(\overline{F_I^0} - \overline{F_M^0}) + 8\pi R\Big(\overline{F_G^0} - \overline{F_M^0}\Big)\Big|_{R=R_c},$$
$$= -8\pi\gamma\Big(\overline{F_I^0} - \overline{F_M^0}\Big),$$
$$= -8\pi\sigma_{MG}(\text{susbstituting Eq. 14}), \quad [15]$$

which is always less than zero, indicating that Type 1 nucleation is a thermodynamically favorable process and ΔF_{T1}^* is maximized at R_c as shown schematically in Fig. 3.

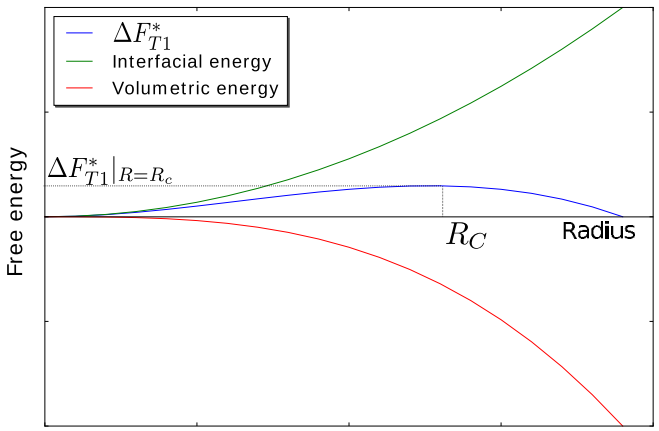

Figure 3. Schematic of the free energy contributions in homogeneous nucleation.

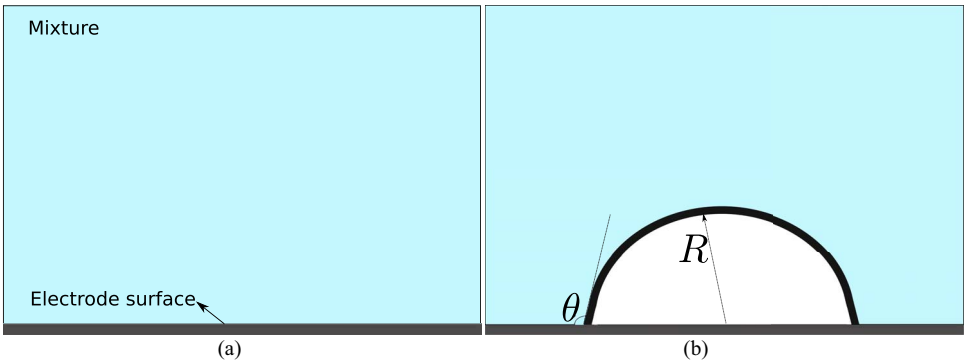

Figure 4. Schematic of heterogeneous nucleation. (a) Before nucleation (b) After nucleation.

The nucleation energy barrier for homogeneous nucleation can be calculated by substituting Eq. 13 in Eq. 12,

$$\Delta F^*_{T1}|_{R=R_c} = \frac{16\pi\gamma^3\left(\overline{F^0_I} - \overline{F^0_M}\right)^3}{3\left(\overline{F^0_G} - \overline{F^0_M}\right)^2}, \quad [16]$$

which is analogous to the classical homogeneous nucleation energy barrier, $\Delta F^*_{T1}|_{R=R_c} = 16\pi\sigma^3_{MG}/(3\Delta G^2_v)$.[18]

Type 2 or heterogeneous nucleation *(T2).*—Fig. 4 shows a schematic of heterogeneous nucleation, where the mixture in contact with the surface forms a gas bubble on an electrode surface with radius R and contact angle θ, measured in the mixture phase.

The geometric parameters to define the bubble like the surface area of the inner surface of interface (A_{MG}), the surface area where solid in in contact with bubble (A_{SG}) and the volume of bubble (V_G) are calculated based on Xu et al.[13] A_{MG} is calculated at the surface with a radius R,

$$A_{MG} = 2\pi R^2\left(1 + \cos\theta\right). \quad [17]$$

Using the above equation, the volume of the interface V_I is determined based on the approximation done is Eq. 7,

$$V_I = \gamma A_{MG} = 2\gamma\pi R^2\left(1 + \cos\theta\right). \quad [18]$$

Similarly A_{SG} and V_G are defined in Eq. 19 and Eq. 20 respectively.

$$A_{SG} = \pi R^2 \sin^2\theta. \quad [19]$$

$$V_G = \pi R^3 \frac{-\cos^3\theta + 3\cos\theta + 2}{3}. \quad [20]$$

The free energy of the system before the nucleation (F^*_1) can be written as

$$F^*_1 = \int_{V_0} F^0_M dV + \int_{A_0} \sigma_{SM} dA. \quad [21]$$

Once the bubble is formed, free energy of the system (F^*_2) is

$$F^*_2 = \int_{V_0 - V_I - V_G} F^0_M dV + \int_{V_I} F^0_I dV + \int_{A_0 - A_{SG}} \sigma_{SM} dA + \int_{A_{SG}} \sigma_{SG} dA + \int_{V_G} F^0_G dV, \quad [22]$$

where the fourth term represents the free energy associated with the sharp solid-gas interface. Although the mixture-gas interface is considered to be diffused, solid-mixture and solid-gas interfaces are considered to be sharp, or zero thickness, to limit the complexity of the model. It should be noted that the effect of solid surface on the diffused interface is neglected in this paper.

The change in free energy of the system (ΔF^*_{T2}) is

$$\Delta F^*_{T2} = \int_{V_0 - V_I - V_G} F^0_M dV + \int_{V_I} F^0_I dV + \int_{A_0 - A_{SG}} \sigma_{SM} dA + \int_{A_{SG}} \sigma_{SG} dA + \int_{V_G} F^0_G dV - \int_{V_0} F^0_M dV - \int_{A_0} \sigma_{SM} dA. \quad [23]$$

Treating volume integrals of F^0_M, F^0_G and F^0_I based on Eq. 4, and considering σ_{SM} and σ_{SG} as constants, Eq. 23 can be written as

$$\Delta F^*_{T2} = V_I\left(\overline{F^0_I} - \overline{F^0_M}\right) - A_{SG}\sigma_{SM} + A_{SG}\sigma_{SG} + V_G\left(\overline{F^0_G} - \overline{F^0_M}\right). \quad [24]$$

Substituting the definition of surface tension at the planar interface σ_{MG} from Eq. 14,

$$\Delta F^*_{T2} = V_I\frac{\sigma_{MG}}{\gamma} - A_{SG}\sigma_{SM} + A_{SG}\sigma_{SG} + V_G\left(\overline{F^0_G} - \overline{F^0_M}\right). \quad [25]$$

Substituting Young's equation for surface wetting for gas bubble, which relates surface tension terms with contact angle as $\sigma_{SG} - \sigma_{SM} = \sigma_{MG}\cos\theta$ (refer to Appendix), into the above equation,

$$\Delta F^*_{T2} = V_I\frac{\sigma_{MG}}{\gamma} + A_{SG}\sigma_{MG}\cos\theta + V_G\left(\overline{F^0_G} - \overline{F^0_M}\right), \quad [26]$$

and finally substituting the definitions of V_I, A_{SG} and V_G through Eqs. 18–20, Eq. 26 can be simplified as

$$\Delta F^*_{T2} = \pi(-\cos^3\theta + 3\cos\theta + 2)\left(\sigma_{MG}R^2 + \frac{R^3}{3}\left(\overline{F^0_G} - \overline{F^0_M}\right)\right). \quad [27]$$

Differentiating the above equation with respect to R gives

$$\frac{d\Delta F^*_{T2}}{dR} = \pi(-\cos^3\theta + 3\cos\theta + 2)\left(2\sigma_{MG}R + R^2\left(\overline{F^0_G} - \overline{F^0_M}\right)\right). \quad [28]$$

The critical radius R_c is always defined by Eq. 13 from classical nucleation theory[18] and this can be verified by equating Eq. 28 to zero. Eq. 28 shows that R_c is independent of contact angle. For nucleation in conical cavities, which is microstructural feature on the electrode surface, critical radius can be shown to be equal to the Type 1 nucleation by redefining the geometric parameters used in this paper.[34] The equivalence of R_c between Type 1 and Type 2 shows that the critical radius required for nucleation is independent of the electrode surface

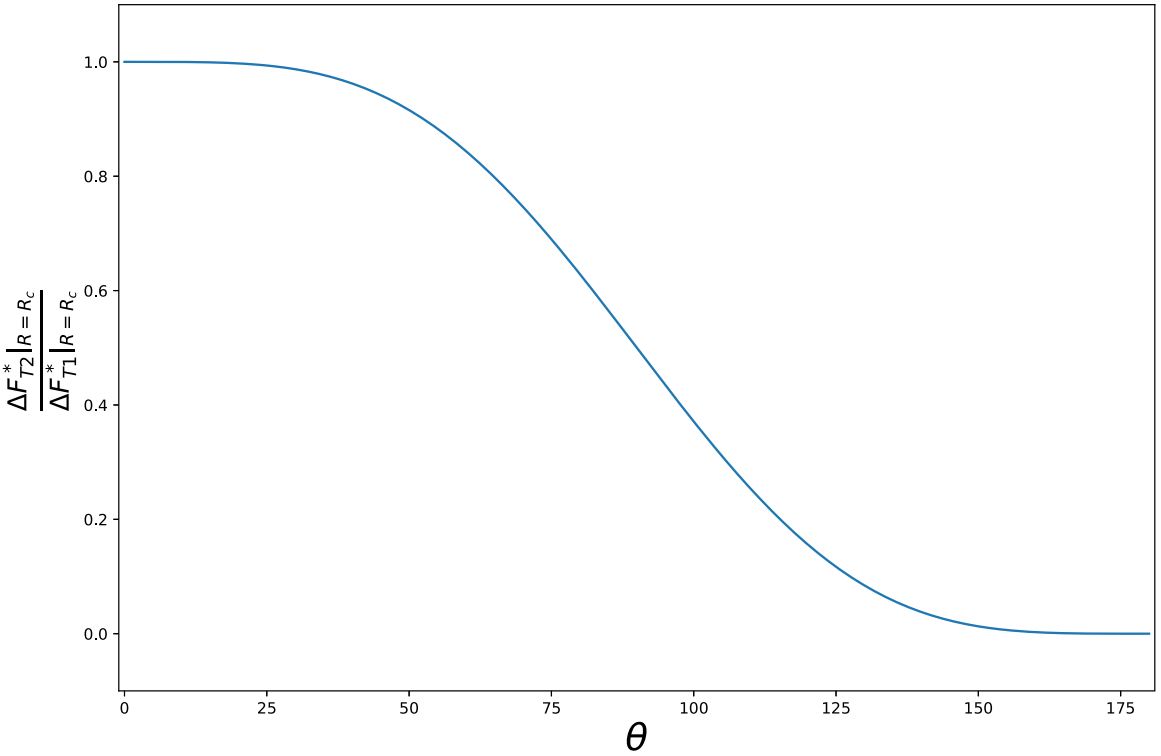

Figure 5. Comparison of the ratio of nucleation energy barrier of heterogeneous and homogeneous nucleation for varying contact angle (in degrees).

properties. The second derivative of ΔF^*_{T2} with respect to R at R_c is

$$\left.\frac{d^2\Delta F^*_{T2}}{dR^2}\right|_{R=R_c} = -2\pi(-\cos^3\theta + 3\cos\theta + 2)\sigma_{MG}, \quad [29]$$

where $-\cos^3\theta + 3\cos\theta + 2 > 0$ for $0 \le \theta \le 180^\circ$, is always less than zero indicating that the ΔF^*_{T2} is maximized at R_c.

The energy barrier for heterogeneous nucleation is

$$\Delta F^*_{T2}|_{R=R_c} = \frac{4\pi\gamma^3\left(\overline{F^0_I} - \overline{F^0_M}\right)^3}{3\left(\overline{F^0_G} - \overline{F^0_M}\right)^2}(-\cos^3\theta + 3\cos\theta + 2), \quad [30]$$

which is analogous to the classical heterogeneous nucleation barrier,[18]

$$\Delta F^*_{T2}|_{R=R_c} = \frac{4\pi\sigma^3_{MG}}{3\Delta G^2_v}(-\cos^3\theta + 3\cos\theta + 2). \quad [31]$$

The ratio between the energy barrier for heterogeneous (Eq. 30) and homogeneous nucleation (Eq. 16) is,

$$\frac{\Delta F^*_{T2}|_{R=R_c}}{\Delta F^*_{T1}|_{R=R_c}} = \frac{-\cos^3\theta + 3\cos\theta + 2}{4}, \quad [32]$$

plotted in Fig. 5. For $\theta = 0^\circ$, $\Delta F^*_{T2}|_{R=R_c} = \Delta F^*_{T1}|_{R=R_c}$ because the nucleated bubble is not in contact with the electrode surface which occurs when the electrode is completely wetted. On the other hand when $\theta = 180^\circ$, $\Delta F^*_{T2}|_{R=R_c} = 0$ (from Eq. 30) corresponds to scenario of a non-wetting mixture and subsequently the bubble covers the surface completely like a film.

Type 3 or pseudo-classical nucleation *(T3)*.—A schematic of the pseudo-classical nucleation mechanism is shown in Fig. 6, where a pre-existing gas bubble of radius R_1 (where $R_1 < R_c$), a metastable state, aids in nucleation of a bubble of radius R.

For the pre-existing bubble, volume of the interface $V_{I,1}$, volume of bubble $V_{G,1}$ and surface area of solid-gas interaction $A_{SG,1}$ are calculated based on the method described in heterogeneous nucleation,

$$V_{I,1} = \gamma A_{MG,1} = 2\gamma\pi {R_1}^2\left(1 + \cos\theta\right),$$
$$V_{G,1} = \pi {R_1}^3\frac{-\cos^3\theta + 3\cos\theta + 2}{3},$$
$$A_{SG,1} = \pi {R_1}^2\sin^2\theta. \quad [33]$$

The volume of the interface V_I, volume of bubble V_G and surface area of solid-gas interaction A_{SG} for the bubble formed after the nucleation are

$$V_I = \gamma A_{MG} = 2\gamma\pi R^2\left(1 + \cos\theta\right),$$
$$V_G = \pi R^3\frac{-\cos^3\theta + 3\cos\theta + 2}{3},$$
$$A_{SG} = \pi R^2\sin^2\theta. \quad [34]$$

The free energy of the system before nucleation (F^*_1) is

$$F^*_1 = \int_{V_0 - V_{I,1} - V_{G,1}} F^0_M dV + \int_{V_{I,1}} F^0_I dV + \int_{A_0 - A_{SG,1}} \sigma_{SM} dA + \int_{A_{SG,1}} \sigma_{SG} dA + \int_{V_{G,1}} F^0_G dV. \quad [35]$$

Correspondingly after nucleation, the free energy of the system (F^*_2) is

$$F^*_2 = \int_{V_0 - V_I - V_G} F^0_M dV + \int_{V_I} F^0_I dV + \int_{A_0 - A_{SG}} \sigma_{SM} dA + \int_{A_{SG}} \sigma_{SG} dA + \int_{V_G} F^0_G dV, \quad [36]$$

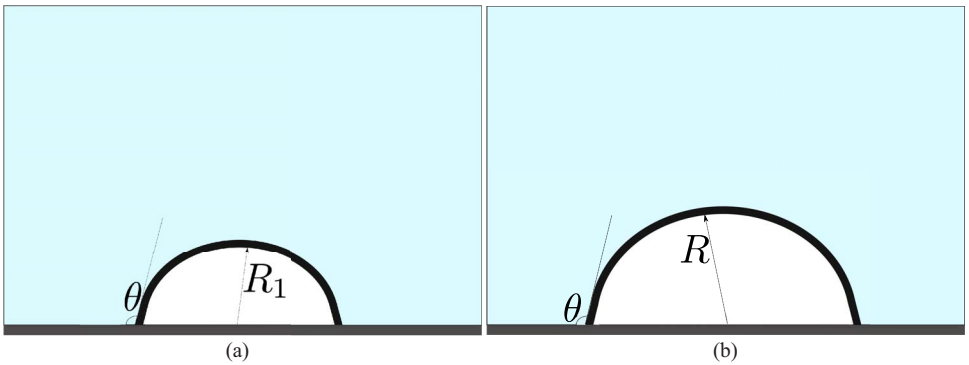

Figure 6. Schematic of pseudo-classical nucleation. (a) Before nucleation (b) After nucleation.

and the change in the free energy (ΔF^*_{T3}) is

$$\Delta F^*_{T3} = \int_{V_0-V_I-V_G} F^0_M dV + \int_{V_I} F^0_I dV + \int_{A_0-A_{SG}} \sigma_{SM} dA + \int_{A_{SG}} \sigma_{SG} dA + \int_{V_G} F^0_G dV - \int_{V_0-V_{I,1}-V_{G,1}} F^0_M dV - \int_{V_{I,1}} F^0_I dV - \int_{A_0-A_{SG,1}} \sigma_{SM} dA - \int_{A_{SG,1}} \sigma_{SG} dA - \int_{V_{G,1}} F^0_G dV. \quad [37]$$

The volume integral of free energies per unit volume (F^0_M, F^0_I and F^0_G) are simplified using Eq. 4, and interfacial tensions between solid-mixture/bubble are considered to be constants. Substituting $V_I - V_{I,1} = \gamma(A_{MG} - A_{MG,1})$ from Eq. 33 and Eq. 34, Eq. 37 can be written as

$$\Delta F^*_{T3} = 2\pi\gamma(1+\cos\theta)(R^2 - {R_1}^2)\left(\overline{F^0_I} - \overline{F^0_M}\right) + \pi\sin^2\theta(R^2 - R_1^2)(\sigma_{SG} - \sigma_{SM}) + \pi\frac{-\cos^3\theta + 3\cos\theta + 2}{3}(R^3 - {R_1}^3)\left(\overline{F^0_G} - \overline{F^0_M}\right). \quad [38]$$

Using the Young's equation for surface wetting and Eq. 14 to simplify the above equation gives

$$\Delta F^*_{T3} = \pi\left(-\cos^3\theta + 3\cos\theta + 2\right)\left(\sigma_{MG}(R^2 - {R_1}^2) + \frac{\overline{F^0_G} - \overline{F^0_M}}{3}(R^3 - {R_1}^3)\right). \quad [39]$$

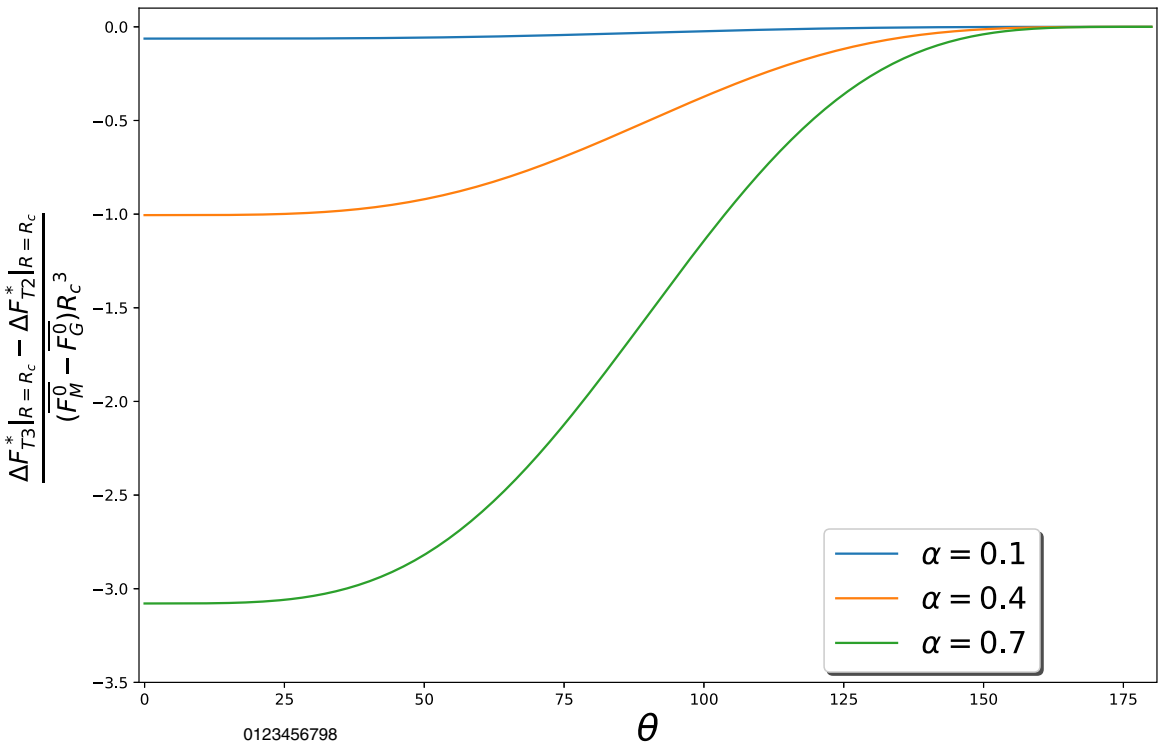

Figure 7. Comparison of normalized nucleation energy between pseudo-classical and heterogeneous nucleation for $0^\circ \leq \theta \leq 180^\circ$ and $\alpha = 0.1, 0.4$ and 0.7.

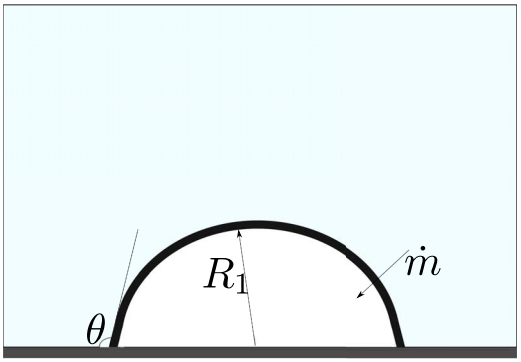

Figure 8. Schematic of non-classical nucleation.

Derivative of Eq. 39 with respect to R is equivalent to Eq. 28, because R_1 is a constant which is independent of nucleation mechanism, and equating it to zero shows that the critical radius for nucleation in Type 3 is also equal to R_c for Type 1 mechanism (Eq. 13). The second derivative of Eq. 39 with respect to R at R_c is Eq. 29, which is always negative, indicating that ΔF^*_{T3} is maximized at R_c.

The nucleation energy barrier for the mechanism is calculated by substituting R_c into Eq. 39,

$$\Delta F^*_{T3}|_{R=R_c} = \pi(-\cos^3\theta + 3\cos\theta + 2)\left(\frac{4\sigma^3_{MG}}{3\left(\overline{F^0_G} - \overline{F^0_M}\right)^2} - \sigma_{MG}{R_1}^2 - \frac{\overline{F^0_G} - \overline{F^0_M}}{3}{R_1}^3\right). \quad [40]$$

In order to compare the nucleation energy barrier of pseudo-classical with heterogeneous nucleation, Eq. 30 is subtracted from Eq. 40,

$$\frac{\Delta F^*_{T3}|_{R=R_c} - \Delta F^*_{T2}|_{R=R_c}}{\overline{F^0_M} - \overline{F^0_G}} = \pi(-\cos^3\theta + 3\cos\theta + 2)\left(-\frac{R_c}{2}{R_1}^2 + \frac{1}{3}{R_1}^3\right). \quad [41]$$

Assuming that $R_1 = \alpha R_c$, where α is an arbitrary real number $0 < \alpha < 1$. Eq. 41 can be rewritten as

$$\frac{\Delta F^*_{T3}|_{R=R_c} - \Delta F^*_{T2}|_{R=R_c}}{\left(\overline{F^0_M} - \overline{F^0_G}\right){R_c}^3} = \pi(-\cos^3\theta + 3\cos\theta + 2)\left(-\frac{1}{2}\alpha^2 + \frac{1}{3}\alpha^3\right), \quad [42]$$

where the left hand side of the above equation can be interpreted as a normalized nucleation energy barrier between pseudo-classical and heterogeneous nucleation. Fig. 7 shows the variation of the normalized nucleation barrier with respect to contact angle θ and α. When $\alpha = 0$, $R_1 = 0$ and $\Delta F^*_{T3}|_{R=R_c} = \Delta F^*_{T2}|_{R=R_c}$ i.e. nucleation energy requirement of Type 3 becomes equivalent to heterogeneous nucleation. With values of α close to unity, R_1 is closer to R_c and the energy barrier for pseudo-classical nucleation also reduces, but it still dependent on the contact angle.

Type 4 or non-classical nucleation *(T4).*—Fig. 8 shows a pre-existing bubble of radius $R_1 \geq R_c$ on a flat electrode surface, which is also a metastable initial state.

The energy barrier for non-classical nucleation can be derived based on the procedure from pseudo-classical nucleation. The nucleation energy barrier required to form a critical nuclei in Type 4 nucleation is described by substituting $R_1 = R_c$ in Eq. 40,

$$\Delta F^*_{T4}|_{R=R_c} = 0, \quad [43]$$

which shows that non-classical nucleation does not require the formation of critical nuclei. The bubble grows by diffusion of gas from the solution, based on mass transfer.[35] Fig. 8 shows the diffusion of gas into the bubble through a mass flux of $\dot{m}$. The diffusion process, which is described by Fick's law, occurs due to the attempt to reduce the free energy gradient across the interface. This process is similar to the growth of the bubble after the nucleation by the previous mechanisms and the change in free energy is driven by the volumetric growth of the bubble. So Type 4 nucleation can be considered as diffusion driven growth which can occur at very low supersaturation levels without the need to form a critical nuclei. Similar diffusion driven nucleation has also been observed and extensively studied during cavitation.[35,36]

Interfacial Free Energy in a Supersaturated Solution

As discussed before, F^0_I does not provide a thermodynamically consistent definition of interfacial energy in a supersaturated solution. In this section, a comprehensive definition of interfacial free energy is derived (from Eq. 14) and shown to be equal to the formulation reported in the literature.

During the analysis of the nucleation mechanisms a description of surface tension between mixture and gas bubble, $\sigma_{MG} = \gamma(\overline{F^0_I} - \overline{F^0_M})$ based on Eq. 14, has been obtained. This along with Eq. 4, can be used to write σ_{MG} as

$$\sigma_{MG} = \frac{\gamma}{V_I}\int_{V_I}\left(k|\nabla\chi_L|^2 + F^0_{mix}\right)dV - \frac{\gamma}{V_0 - V_I - V_G}\int_{V_0 - V_I - V_G} F^0_M dV. \quad [44]$$

Since $V_0 >> V_I + V_G$ and composition of mixture bulk (away from the nucleated bubble) is constant, volume averaged F^0_M can be approximated to be equal to $F^0_M|_{r\to\infty}$. Eq. 44 can be rewritten as

$$\sigma_{MG} = \frac{\gamma}{V_I}\int_{V_I}\left(k|\nabla\chi_L|^2 + F^0_{mix} - F^0_M|_{r\to\infty}\right)dV. \quad [45]$$

For a flat or planar interface (when $R \to \infty$), Eq. 45 can be written as

$$\sigma_{MG} = \int_{\gamma}\left(k|\nabla\chi_L|^2 + F^0_{mix} - F^0_M|_{x\to\infty}\right)dx. \quad [46]$$

If the above integral is computed locally anywhere within the entire system but it would be non-zero only when the composition changes near the interface.[20] So Eq. 46 can also be written as

$$\sigma_{MG} = \int_{-\infty}^{\infty}\left(k|\nabla\chi_L|^2 + F^0_{mix} - F^0_M|_{x\to\infty}\right)dx, \quad [47]$$

which is the surface tension of the planar interface in a supersaturated solution. The work by C-H[20] also derives Eq. 47 as the surface tension in a supersaturated solution. The interfacial energy (F^*_{MG}) can be written as a local volume (v) integral (based on the formulation of surface tension Eq. 47)

$$F^*_{MG} = \int_{v}\left(k|\nabla\chi_L|^2 + F^0_{mix} - F^0_M|_{x\to\infty}\right)dV, \quad [48]$$

which is used as the interfacial energy in the presence of a supersaturated solution in the work by C-H on nucleation.[20] The formulation of F^*_{MG} (Eq. 48) and σ_{MG} (Eq. 47) becomes zero outside the interface region in the presence of supersaturated mixture as shown by C-H.[20]

Discussion

Although the critical radius is independent of the nucleation mechanism the nucleated bubble volume is different in each mechanism, with the bubble produced during homogeneous nucleation being largest compared to heterogeneous and pseudo-classical nucleation while non-classical nucleation does not require formation of one. The nucleation energy barrier is highest in homogeneous nucleation, which indicates the high levels of supersaturation required for this

mechanism. In heterogeneous nucleation, the nucleation energy barrier is lower than homogeneous nucleation, but it is dependent on the contact angle (Eq. 30). In case of pseudo-classical nucleation, the presence of pre-existing gas bubble reduces the nucleation energy barrier compared to heterogeneous nucleation (as seen in Eq. 40). The smaller the pre-existing bubble, the closer the nucleation energy barrier of this process is to heterogeneous nucleation. On the other hand, if the radius of the pre-existing bubble is close to critical radius, the nucleation energy barrier of the pseudo-classical mechanism is very small. When the pre-existing bubble has a radius larger than the critical radius (non-classical nucleation), the nucleation energy barrier is negligible because the formation of critical nuclei is not necessary. This mechanism is the mode of growth of all the nucleated bubbles, which involves diffusion of gas into the bubble from the supersaturated mixture.

The importance of contact angle in determining energy barrier associated with heterogeneous and pseudo-classical nucleation is shown in Fig. 7. When $\theta = 180^{\circ}$, the energy barrier of both the heterogeneous and pseudo-classical nucleation mechanisms are negligible, i.e. the surface of the electrode is non-wetting or hydrophobic thus promoting gas evolution, as observed in the work by Kadyk et al.[25] On the contrary, when $\theta = 0^{\circ}$, $\Delta F^*_{T2}|_{R=R_c} = \Delta F^*_{T1}|_{R=R_c}$ and $\Delta F^*_{T3}|_{R=R_c} < \Delta F^*_{T2}|_{R=R_c}$. The difficulty of nucleating gases on a hydrophilic surface, has been experimentally observed in the work by Yang et al.[37] So if there is no pre-existing bubble on the hydrophilic electrode surface, homogeneous nucleation is thermodynamically more favorable than heterogeneous mechanism. In the presence of a pre-existing bubble, pseudo-classical or non-classical nucleation is more probable than both homogeneous and heterogeneous mechanisms.

The free energy of the mixture (F^0_M) varies non-linearly with respect to composition (χ_L), usually described by a double well function.[19,20,26] When $\overline{F^0_M} - \overline{F^0_G}$ is written equal to ΔG_v, Eq. 14, an additional term which arises due to the non-linear variation of the F^0_M with respect to χ_L should also be considered, as done by C-H.[20] This term can be written as

$$\delta F^0 = \left(\chi_L|_{r\to 0} - \chi_L|_{r\to\infty}\right)\frac{dF^0_{mix}}{d\chi_L}\bigg|_{\chi_L|_{r\to\infty}},$$

and ΔG_v can be redefined accordingly as $\overline{F^0_M} - \overline{F^0_G} + \delta F^0$. Since this paper does not describe variation of the free energy of the mixture with respect to composition, this term was not included while describing ΔG_v (Eq. 14).

In the work by C-H[19,20] and Lee et al.,[26] F_{mix} is considered to be equal to ΔF^0, because the relative change in the thermodynamic values for the given state is considered instead of its absolute values. Using this approximation will alter only the definitions of free energy per unit volume of states but would not influence the method used or derived conclusions. Using this definition of the free energies, Eq. 47 become equivalent to the formulation derived in Ref. 19 when the mixture is not supersaturated or $F^0_M|_{x\to\infty} = 0$. And the critical radius calculated in Eq. 13 can be shown equivalent to the formulation of critical radius derived by C-H.[20] A complete definition of the interfacial free energy in a supersaturated solution, given by Eq. 48, is derived from the thermodynamic definition of the system. This definition of the interfacial energy is analogous to the description used by C-H in their work on nucleation in supersaturated solutions.[20] Further investigation of the surface tension description for a planar interface (Eq. 47) was performed by C-H.[20]

Conclusions

A thermodynamical explanation of nucleation mechanisms is successfully developed using Helmholtz free energy change of the system. The Type 1 and Type 2 nucleation energy barriers obtained from this analysis are analogous to the energy requirement in the classical theories. Even though the critical radius for the formation of the nuclei is equal for all mechanisms, there is a substantial difference in the nucleation energy barrier between the mechanisms. Homogeneous nucleation has the largest nucleation energy barrier, followed by heterogeneous nucleation, then pseudo-classical nucleation. The non-classical nucleation is a bubble growth mode, as it does not require formation of critical nuclei. The pre-existing bubble on the electrode surface has been observed to reduce the nucleation energy barrier, based on its radius. The contact angle has also shown to play an important role in the nucleation energy for heterogeneous and pseudo-classical nucleation mechanisms. It has been shown that value of contact angle can thermodynamically favor one mechanism over the other. A definition of surface tension for planar interfaces that depends on the Helmholtz free energy of the mixture has also been determined from the thermodynamic framework which is found in the literature.

Acknowledgment

The authors acknowledge the discussions with Dr. Maria Fernandino (NTNU) about the C-H formulation used in the work by Lee et al.[26] We would also like to thank the Department of Material Science and Engineering, NTNU, for funding this research.

Appendix: Contact Angle Derivation for Gas Bubbles

The contact angle plays an important role in the balance between the surface energies of the gas bubble. In this section, the contact angle is derived from the free energy of the system based on the work by Bormashenko and Gendelman, who derived the Lippman equation of a liquid droplet from its free energy description.[38]

From heterogeneous nucleation, the free energy of the system, F^*_2 (from Eq. 22), is written as

$$F^*_2 = \int_{V_0-V_I-V_G} F^0_M dV + \int_{V_I} F^0_I dV + \int_{A_0-A_{SG}} \sigma_{SM} dA + \int_{A_{SG}} \sigma_{SG} dA + \int_{V_G} F^0_G dV. \quad [A1]$$

Using Leibniz formula to differentiate the above integral,

$$dF^*_2 = \overline{F^0_M} d(V_0 - V_I - V_G) + \overline{F^0_I} dV_I + \sigma_{SM} d(A_0 - A_{SG}) + \sigma_{SG} dA_{SG} + \overline{F^0_G} dV_G. \quad [A2]$$

Writing V_I as γA_{MG} and considering only the surface energy contributions, as the contact angle is determined by the balance in surface energy rather than the volumetric energy terms,

$$dF^*_2 = \gamma(\overline{F^0_I} - \overline{F^0_M}) dA_{MG} - \sigma_{SM} dA_{SG} + \sigma_{SG} dA_{SG}. \quad [A3]$$

And with the definition of σ_{MG} (Eq. 14) and $dF^*_2 = 0$, Eq. A3 can be rewritten as

$$-\sigma_{MG} dA_{MG} = (\sigma_{SG} - \sigma_{SM}) dA_{SG}. \quad [A4]$$

Substituting $dA_{MG} = -\cos\theta dA_{SG}$, the $-$ is a result of $\cos(\pi - \theta) = -\cos\theta$,

$$\sigma_{MG}\cos\theta = \sigma_{SG} - \sigma_{SM}, \quad [A5]$$

which is the Young's equation for gas bubbles, with contact angle defined in the mixture phase.

ORCID

Kurian J. Vachaparambil http://orcid.org/0000-0001-7425-9291

References

1. T. Yamamoto and M. Matsumoto, *J. Therm. Sci. Technol.*, **7**(1), 334 (2012).
2. H. Vogt, Ö. Aras, and R. J. Balzer, *Int. J. Heat Mass Transfer*, **47**(4), 787 (2004).
3. S. F. Jones, G. M. Evans, and K. P. Galvin, *Adv. Colloid Interface Sci.*, **80**(1), 27 (1999).
4. N. J. Hepworth, J. W. R. Boyd, J. R. M. Hammond, and J. Varley, *Chem. Eng. Sci.*, **58**(17), 4071 (2003).
5. A. K. Biń, *Chem. Eng. Sci.*, **48**(21), 3585 (1993).
6. S. G. Bankoff, *AIChE J.*, **4**, 24 (1958).
7. P. Attard, *Langmuir*, **32**(43), 11138 (2016).
8. S. R. German, M. A. Edwards, Q. Chen, Y. Liu, L. Luo, and H. S. White, *Faraday Discuss.*, **193**, 223 (2016).
9. C. A. C. Sequeira, D. M. F. Santos, B. Šljukić, and L. Amaral, *Braz. J. Phys.*, **43**(3), 199 (2013).
10. A. Taqieddina, R. Nazarib, L. Rajicb, and A. Alshawabkeh, *J. Electrochem. Soc.*, **164**(13), E448 (2017).

11. K. E. Einarsrud and S. T. Johansen, *Prog. Comput. Fluid Dyn.*, **12**(2–3), 119 (2012).
12. P. Maciel, T. Nierhaus, S. V. Damme, H. V. Parys, J. Deconinck, and A. Hubin, *Electrochem. Commun.*, **11**(4), 875 (2009).
13. W. Xu, Z. Lan, B. Peng, R. Wen, and X. Ma, *RSC Adv.*, **5**(2), 812 (2015).
14. S. K. Singha, P. K. Das, and B. Maiti, *J. Chem. Phys.*, **143**(20), 204703 (2015).
15. K. E. Einarsrud, I. Eick, W. Bai, Y. Feng, J. Hua, and P. J. Witt, *Appl Math Model.*, **44**, 3 (2017).
16. S. D. Lubetkin, *Langmuir*, **19**(7), 2575 (2003).
17. S. Jain and L. Qiao, *AIP Adv.*, **7**(4), 045001 (2017).
18. K. F. Kelton and A. L. Greer, *Nucleation in Condensed Matter: Applications in Materials and Biology*, p. 27, 28, 173, Pergamon Materials Series, Amsterdam (2010).
19. J. W. Cahn and J. E. Hilliard, *J. Chem. Phys.*, **28**, 258 (1958).
20. J. W. Cahn and J. E. Hilliard, *J. Chem. Phys.*, **31**, 688 (1959).
21. H.-J. Butt, K. Graf, and M. Kappl, *Physics and Chemistry of Interfaces*, p. 29-41, Wiley-VCH Verlag GmbH & Co. KGaA, Weinheim (2006).
22. H. Vogt, *Electrochem. Acta*, **29**(2), 167 (1984).
23. P. Vassie and A. C. C. Tseung, *Electrochem. Acta*, **20**, 759 (1975).
24. P. Vassie and A. C. C. Tseung, *Electrochem. Acta*, **20**, 763 (1975).
25. T. Kadyk, D. Bruce, and M. Eikerling, *Sci. Rep.*, **6**, 38780 (2016).
26. D. Lee, J.-Y. Huh, D. Jeong, J. Shin, A. Yun, and J. Kim, *Comp. Mater. Sci.*, **81**, 216 (2014).
27. A. J. M. Yang, P. D. Fleming III, and J. H. Gibbs, *J. Chem. Phys.*, **64**, 3732 (1976).
28. P. Yue, J. J. Feng, C. Liu, and Jie Shen, *J. Fluid Mech.*, **515**, 293 (2004).
29. F. Boyer, C. Lapuerta, S. Minjeaud, B. Piar, and M. Quintard, *Transport Porous Med.*, **82**(3), 463 (2010).
30. S. Keßler, F. Schmid, and K. Drese, *Soft Matter*, **12**(34), 7231 (2016).
31. A. J. Ardell, *Scripta Mater.*, **66**(7), 423 (2012).
32. F. S. Cipcigan, V. P. Sokhan, A. P. Jones, J. Crain, and G. J. Martyna, *Phys. Chem. Chem. Phys.*, **17**, 8660 (2015).
33. T. Ito, H. Lhuissier, S. Wildeman, and D. Lohse, *Phys. Fluids*, **26**, 032003 (2014).
34. L. Xiang-Ming, *Chinese Phys. Lett.*, **31**, 038201 (2014).
35. T. F. Groß, J. Bauer, G. Ludwig, D. Fernandez Rivas, and P. F. Pelz, *Exp. Fluids*, **59**(1), 12 (2018).
36. T. F. Groß and P. F. Pelz, *J. Fluid Mech.*, **830**, 138 (2017).
37. J. Yang, J. Duan, D. Fornasiero, and J. Ralston, *J. Phys. Chem. B*, **107**(25), 6139 (2003).
38. E. Bormashenko and O. Gendelman, *Chem. Phys. Lett.*, **599**, 139 (2014).